Behaviour of the Stiffened Panels of Rectangular Industrial Ducts

K.S.Sivakumaran
Department of Civil Engineering, McMaster University, Hamilton, Ontario, Canada L8S 4L7
siva@mcmaster.ca

T. Thanga
Hatch Ltd, Mississauga, Canada
TThanga@hatch.ca

B. Halabiah
BAH Enterprises Inc., Canada
bhalabieh@bahinc.ca

Abstract
Large rectangular industrial duct side panels often require regularly spaced stiffeners. Generally, the stiffeners are wide flanged steel beam sections with one flange connected to the steel panel and the other flange unsupported and unbraced. Under negative pressure (suction), the unconnected flange is in compression and the duct panel is in tension. The duct panel and the web to which the tension flange is connected they may provide a partial rotational restraint to the compression flange. This investigation concerns with the bending capacity and the design of such stiffened steel panels. Finite element analysis models for stiffened steel panels were built and this paper describes the features of this model and presents the convergence study results. The shell elements can model thick and thin shell structures, undergoing large displacement/small strains. The material model was elasto-plastic-multilinear material model with von Mises yield criterion. The model included geometric imperfections and residual stresses. The Load Displacement Control (LDC) method was used to capture the loading and unloading regions of the pressure load-lateral deflection response. Based on the comparison of results with the corresponding experimental results, it was concluded that the as built finite element analysis model can reliably establish the response of stiffened plates in the loading and in the unloading branches.

Keywords
Rectangular duct, Stiffened Plates, Finite element method, Stiffener Buckling, Bending strength

1. Introduction
Many heavy industrial processes require transport of large amount of high pressure air or other gases through series of steel ducts. The duct structural systems associated with such industrial applications are significantly large and in some ways are quite unique structures. Though ducts having circular or rectangular cross-sections are feasible, rectangular cross-sectional ducts are commonly used in large industrial applications. The cross-sectional dimensions of such industrial rectangular ducts may be in the range of 5 m to 15 m. Figure 1 shows an industrial duct during fabrication. The rectangular cross-section is formed by welding together relatively thin steel plates. These side plates are generally stiffened with parallel configuration stiffeners. The positive or negative pressure inside the ducts may be in the range of 10 to 15 kPa. The governing load combination due to internal pressure, wind load and other loads may be

in the range of 15 to 20 kPa. The strip of plate between parallel stiffeners is assumed to span and be supported by those stiffeners. Thus, in duct structural system the load path is from the plate to the stiffeners. The selection of plate thickness goes hand in hand with the stiffener spacing. For a given plate thickness, however, the stiffener spacing is determined by considering the allowable stress and deflection of a unit width of plate strip between stiffeners. The allowable stress and deflection of the strip of the plate is generally calculated by considering the large deflection plate theory to include the bending stress and diaphragm stress. This paper concerns with the behavior and design of stiffeners.
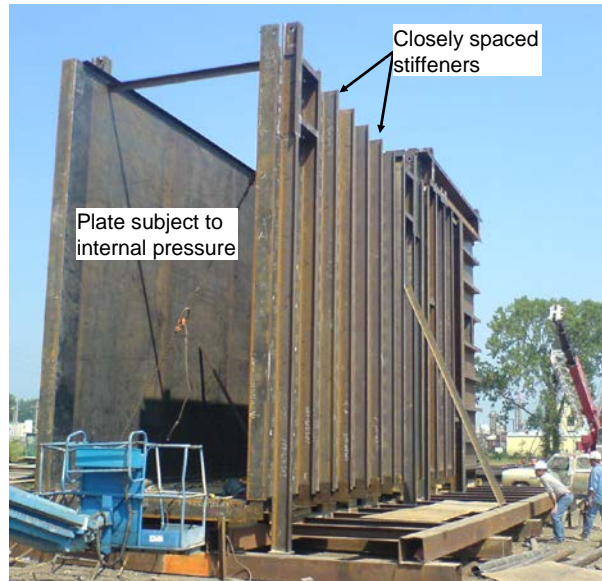
Figure 1: An industrial duct during fabrication

2. Behavior and the Capacity of the Stiffener

In view of the size and in view of the high loading, often, wide flanged structural sections are used as stiffeners, where one of flanges is weld connected to the plate, whereas the other flange is unbraced and unsupported. When the duct is under the active pressure, the unconnected flange would be in tension and the connected flange and the plate would be in compression. This situation is often not critical and easier to accommodate, though an effective width of the plate between the stiffeners needs to be considered. However, when the duct is under suction (negative pressure) the unconnected/unbraced flange would be in compression and the connected flange and the plate would be in tension. Under such loading, the lateral-torsional buckling of the stiffener may govern the strength of the stiffened panel. Figure 2 shows the general arrangement of the stiffened panel under suction and the repetitive pattern a structural engineer may consider for analysis and design the stiffener.
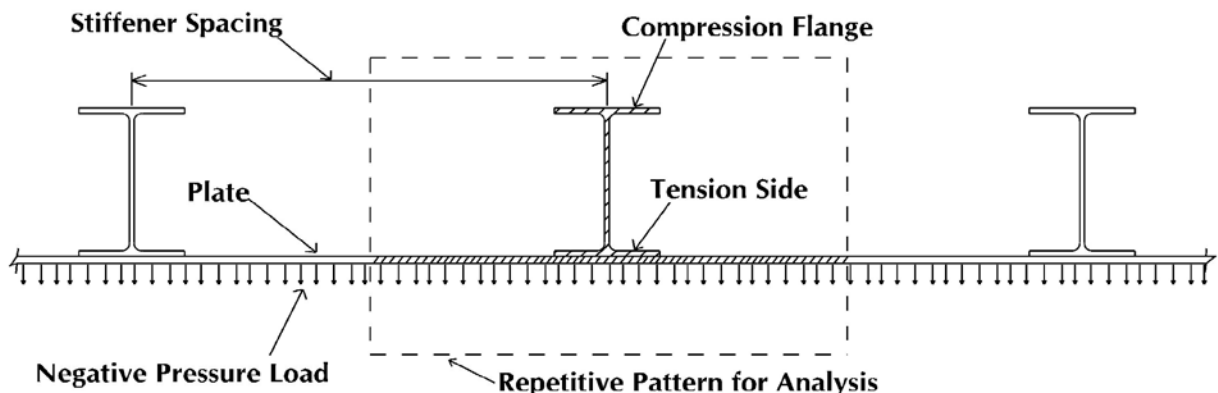
Figure 2: General Arrangement of the Stiffened Panel and the Repetitive Pattern

968

In view of the combination of the I-section and the plate panel, the repetitive pattern results in a singly symmetric section. The shear center and the centroid do not coincide in such singly symmetric sections. For such sections bent about the symmetric axis, the lateral-torsional buckling moment is given by the formula (Galambos, 1998);

$$M_{cr} = \frac{C_b \pi^2 EI_y \beta_x}{2(K_y L_b)^2}\left[1 \pm \sqrt{1 + \frac{4}{\beta_x^2}\left[\frac{C_w K_y^2}{I_y K_z^2} + \frac{GJ(K_y L_b)^2}{\pi^2 EI_y}\right]}\right]$$

(1)

Where, E and G are the modulus of elasticity and rigidity, respectively, I_y -minor axis second moment of area, J -St.Venant torsional constant, C_w -warping constant, L_b -unbraced length of the beam, K_y and K_z are the effective length factors depending on the lateral and warping end restraints, C_b is the equivalent uniform moment factor, and β_x is the mono-symmetry coefficient. For practical purposes β_x of the repetitive section shown in Figure 2 can be approximated by;

$$\beta_x = 0.9d'\left(\frac{2I_{yc}}{I_y} - 1\right)\left(1 - \left(\frac{I_y}{I_x}\right)^2\right)$$

(2)

where the d' is the distance between the centres of areas of the flanges, and I_x and I_y are the second moment of areas of the whole section with respect to major and minor axis, respectively, and I_{yc} is the minor axis second moment of area of the compression flange (Kitipornchai and Trahair, 1980). In reality though, the stiffeners of the industrial duct may be treated as fully restrained against lateral translation and perhaps elastically restrained against twist. Under this scenario, the stiffener may undergo elastic or inelastic distortional buckling of the web than overall lateral-torsional buckling. Closed form solutions, similar to equation (1), are not easy to derive for this case because of the complexity of distorted cross section. Approximate critical moment corresponding to such web distortional buckling may be established based on the assumption that compression flange is a uniformly stressed strut restrained by a continuous translational restraint provided by the web. In this approach, the uniformly stressed flange is translationally restrained by a continuous restraint of stiffness α per unit length. Then, the elastic buckling load can be derived as;

$$N_{cr} = (\pi^2 EI_f/L^2) + \alpha L^2/\pi^2$$

(3)

where EI_f is the flexural rigidity of compression flange and L is the length of the strut. The minimum value of N_{cr} may be obtained by differentiating the above equation with respect to L. The elastic buckling load can then be used to determine the elastic critical moment. The method was extended for varying axial force on the compression flange by Svensson (1985) but it has been shown to predict the elastic critical load inaccurately for rolled beams (Bradford, 1998)

Various researchers have built beam type finite elements to capture the web distortional buckling of beams. Hancock, et.al. (1980) considered a two node four degrees of freedom element consisting of rigid body translations (U_T and U_B) and the twists ($\emptyset_T$ and $\emptyset_B$) of top and bottom flanges. The web was assumed to be distorted into a cubic curve, whereas the deflections and twists varied sinusoidally along the length of member. Bradford and Trahair (1981) extended the element to have six nodel out-of-plane buckling degrees of freedom, comprising the two flange translations U_T and U_B, two flange rotations U_T' and U_B' and two flange twists about vertical axis $\emptyset_T$ and $\emptyset_B$. Thus, this beam type finite element has six degrees of freedom at each node. Bradford (1988) considered monosymmetric beams, where top and bottom flange strain energies due to warping and twisting of flanges were calculated separately. These studies were further extended to include the inelasticity using an incremental and iterative solution of buckling. Here, tri-linear stress-strain curve and linear residual stress pattern were assumed for the structural steel. Bradford (1999) considered continuous elastic restraints against translation, minor axis rotation, torsion and warping, which yielded a beam type finite element that incorporates eight degrees of

freedom per node, namely, U_T, U_B, $U_T{'}$, $U_B{'}$, $\emptyset_T$, $\emptyset_B$, $\emptyset_T{'}$ and $\emptyset_B{'}$, where prime indicates the rate of change with respect the longitudinal axis. However, such beam type finite element models require correct global boundary stiffness values associated with the elastic restraints. Furthermore, with the available plate/shell finite element and the computing power more precise modeling of stiffened steel plate panels can be achieved, where factors such as residual stresses and initial imperfections can be explicitly incorporated into the numerical models. Next section describes such a finite element model built for this study using the commercially available, multi-purpose finite element software package ADINA (2009). The performance of the model was verified by comparing the predicted responses with the test results.

3. The Finite Element Analysis Model for Stiffened Plates of Industrial Ducts

The finite element analysis method can be conveniently used to accurately trace the buckling behaviour of stiffened plate panels. In addition to obtaining their buckling and collapse modes, the finite element analysis will give the deformations and stresses of a stiffened plate panel subjected to pressure loads. The stiffeners in the duct are equally spaced along the surface and span on the sides of the industrial duct. Because of the symmetry of stiffeners, only one repetitive panel as shown in Figure 2, i.e. a portion of the plate of width b with the stiffener centered on the plat strip, need to be modeled. The large deflection of laterally loaded stiffened plate panel involves in-plane and out-of-plane displacements. Therefore, shell element was used to study the behavior of the laterally loaded plate. The 4-node nonlinear shell element with the shell mid-surface nodal points was formulated with the assumptions used in the Timoshenko beam theory and the Mindlin/Reissner plate theory. The shell element used in this study can be employed to model thick and thin general shell structures, undergoing large displacement/small strains. The material model selected for the elements was elasto-plastic-multilinear material model with von Mises yield criterion, associated flow plasticity based on isotropic hardening rule. In order to capture the onset and spread of material yielding through thickness the Newton-Cotes rule with seven integration points was chosen. The Load Displacement Control (LDC) method of ADINA(2009) was used to capture the loading and unloading regions of the pressure load-lateral deflection response. The LDC method uses the load magnitude as the unknown and controls the incremental displacement from the load-displacement response. This method will terminate the computations at a user defined displacement.

Initial Geometric Imperfections: The initial geometric imperfections may exist in plate elements of stiffened plate panels. These imperfections arise during the production of stiffeners and welded fabrication of the stiffened plate. Furthermore, the finite element based buckling analysis needs some disturbance (geometric or load) in order to initiate the buckling. Therefore, the current study incorporated a double sine wave geometric imperfection. In general, the lines of web/flange intersections were defined to be straight, and either the middle line or the free edges along the length direction was defined to form a number of half sine waves. Figure 3 shows the resulting geometric imperfections. The Canadian standard for general requirements structural quality steel (CISC, 2010) permits a maximum variation in straightness of the plate of 0.001 times of length of half sine wave, which was assigned here as the peak imperfection.

Exaggarated Sinusoidal Initial Geometric Imperfection
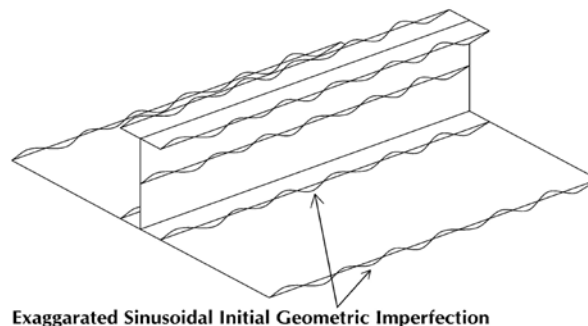
Figure 3: Geometric Imperfections

Residual Stresses: In W-shaped members, such as the stiffeners, due to hot rolling and sudden cooling the tips of the flanges and the center of the web experience compressive residual stresses while the flange-to-web junctions experience tensile residual stresses. Residual stresses are self equilibrating stresses and for this analysis the stiffener residual stresses were taken to be of a linear pattern with a peak compressive and tensile stresses of $0.3F_y$, where F_y is the yield strength. The welding operations cause tensile stresses at the weld location and compressive stresses in adjacent areas. Staggered intermittent fillet welds are widely used in industrial ducts to connect the flange tip of the stiffener to the plate. In this analysis, a linearly varying tensile stresses (peak value of $0.5F_y$) were assumed to exist in the plate to a distance of $b_f/6$ on either side of the flange tip, where, b_f is the flange width of the stiffener. Equilibrating compressive stresses were assumed to be of uniform distribution of value $0.125F_y$ over a distance of $b_f/3$ on either side of the tensile stresses. The residual stresses were incorporated into the FE model as initial strains at nodal points.

Material Model: The material model used for this study was a tri-linear representation where, the elastic-plastic-strain hardening behavior was idealized considering three distinct material stress-strain relationship featuring; initial linear portion, yield plateau, and a linear strain hardening portion. The study considered A992 and 44W steel grades, and the Young Modulus E for both steel grades was taken as 200 GPa, however, the yield stresses were assumed to be 345MPa and 300MPa, respectively, giving a corresponding yield strains of 0.001725 and 0.0015, respectively. The strains at initiation of strain hardening for these steel grades were taken as twenty times the yield strain, thus, they were 0.0345, and 0.03, respectively. The strain hardening slope E_{st} was considered to be (E/30 = 6.67GPa). The ultimate strength of A992 and 44W steel grades were taken to be 450 MPa, and 400MPa, respectively. The other parameter considered herein is Poisson's ratio υ, whose value for steel is 0.3. Beyond ultimate stress, a large value of fracture strain was specified, which may never be reached in the analysis.

Mesh density and Convergence Study: In order to establish a suitable mesh density for this numerical study, a convergent study was performed. Insert in Table 1 shows the model of the stiffened plate panel used in this mesh size convergent study. The thickness of the plate was 5mm and was assumed to be made by ASTM A36 steel having 250MPa nominal yield strength. The I-shaped stiffener was chosen to be 200mm deep. The stiffener section was assumed to be made by ASTM A992 steel having yield strength of 345 MPa. The stress-strain relations of both materials were idealized to be a tri-linear. The sinusoidal geometric imperfection (δ_o/b=0.001) was used. The stiffened plate panel was subjected to suction type negative pressure. The moment at the mid-span, which can be calculated based on the pressure and plate dimensions, was monitored for increasing pressure. Five different finite element mesh configurations were considered in this convergence study. The coarse mesh contained only 1120 shell elements, whereas the most refined mesh contained 5920 elements. The Table 1 shows the mesh details and the analysis results, including percentage change associated with the ultimate moment resistance. The percentage change in ultimate moment resistances between mesh density of 1 & 2, 2 & 3 and 3 & 4 were 5.32 %, 2.03 % and 1.41 % respectively. The percentage change in the ultimate moment between mesh density of 4 and 5 was only 0.38 %.In general, the percentage change less than 5 % may be considered acceptable. Thus, mesh density 2, 3, 4 and 5 may be acceptable. However, due to the severe nature of the material and geometric nonlinearities involved in the current analyses, a very dense mesh of shell elements was desirable in order to trace the nonlinear equilibrium path into the unloading regime. Thus, mesh 5 was selected as the most suitable mesh and this mesh density was used for rest of the studies presented in this paper. In Physical dimensions, each element in this mesh is of size 50 mm x 20 mm.

Table 1: Mesh Density and Convergence Study
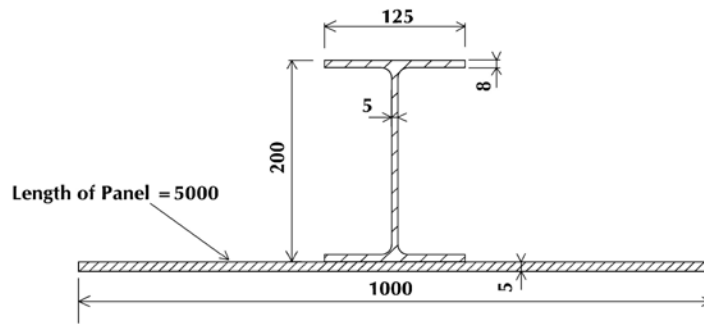
Mesh Number	Physical Size (mm x mm)	Number of Elements	M_{ult} (kN.m)	Percentage Change / (%)
1	125x65	1120	115.23	
2	108x31	1656	109.41	-5.32
3	100x30	2300	107.23	-2.03
4	83x21	3840	105.74	-1.41
5	50x20	5920	105.34	-0.38

4. Verification of the Finite Element Model

Prior to application of the proposed finite element models in parametric studies the model was applied to an experimental study on such stiffened plates by Udall(2007). The scope of that study was to establish the experimental capacity. To simulate the loading and the boundary condition of industrial duct, a shallow box with removable top was made. The removable top contained the plate with a stiffener. The box was made air tight and was subjected to vacuum pump caused suction pressure load. This arrangement simulated a single stiffener and plate between adjacent stiffeners subjected to lateral pressure. The size of the box was 4572mm x 2438mm in plan area and 152mm deep. The thickness of plate of stiffened panel was 4.76 mm and made of ASTM 44W steel having 300MPa nominal yield strength. The test stiffeners were W8x18 and W12x14 wide flange sections made of A992 steel having 345MPa nominal yield strength. The stiffeners W8x18 and W12x24 were considered compact and slender sections, respectively, which may cause different failure modes. The experiment was repeated three times.

Two finite element models for stiffened plate panels, each for stiffeners W8x18 and W12x14, were developed to validate the accuracy of the model using the experiment results. All degrees of freedom for all nodes were set to freely translate and rotate, except at the nodes along the four edges of the plate where they were constraint against translations and rotations, thereby creating fixed boundary conditions. The out-of-plane and in-plane lateral translation of flange and web of the stiffeners were not prevented during the experiment to create the case of an actual structure. The Load Displacement Control (LCD) method was used to follow the nonlinear equilibrium path of the model until it collapse. The analytical and experimental results for stiffened plate panel of stiffener W8X18 and W12x14 are shown in Figure 4. The vertical and horizontal axes represent the pressure load in kPa and mid-span deflections in mm, respectively. It could be observed that the FE analysis results agree very well with the experimental results. The shapes of the curves are similar and the measured and the predicted peak strengths are almost same. The differences between the predicted capacities and measured capacities are 1% for the stiffener W8x18 and only 7% for the stiffener W12x14. The numerical model of stiffener W8x18 buckled when the mid-span vertical deflection reached around 30 mm, however, the buckling at the experiment occurred gradually after the mid-span vertical deflection of 30 mm. This could be most likely due to the fact that the vacuum box was distorted during the experiment. The other reason might be due to the slip during the

experiment between the plate and the vacuum box, whereas in the finite element model the plate was assumed to be rigidly connected. The numerical results show the increment in the pressure beyond buckling, which is because of the membrane action in plate which becomes significant after stiffener buckling. The buckling modes corresponding to experiments and the numerical analysis are shown in Figure 5. It could be noted that both experimental and numerical models failed in similar buckling modes, i.e. the failure was more ductile nature as expected. Despite minor differences, it could be concluded that the finite element analysis model could be relied on the response of loading and unloading branches.
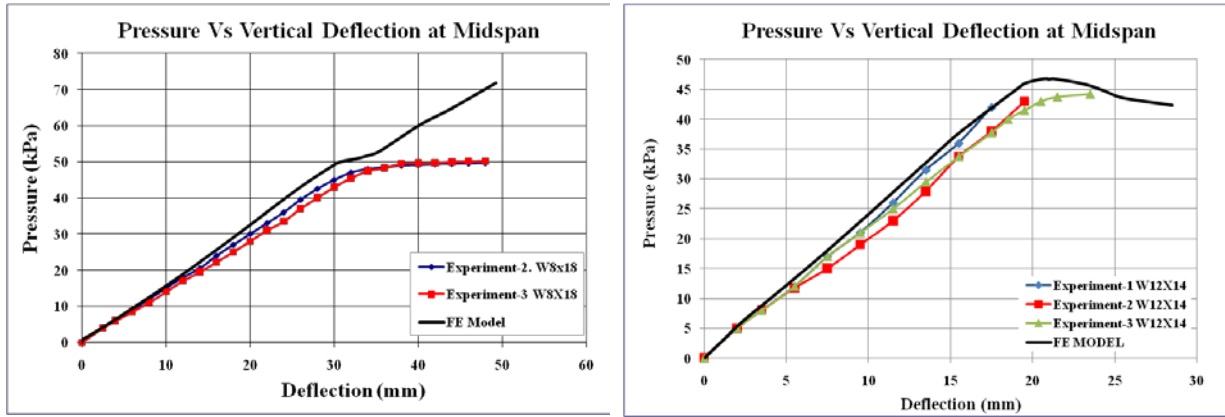
Figure 4: Internal Pressure versus Vertical Deflection Relationship
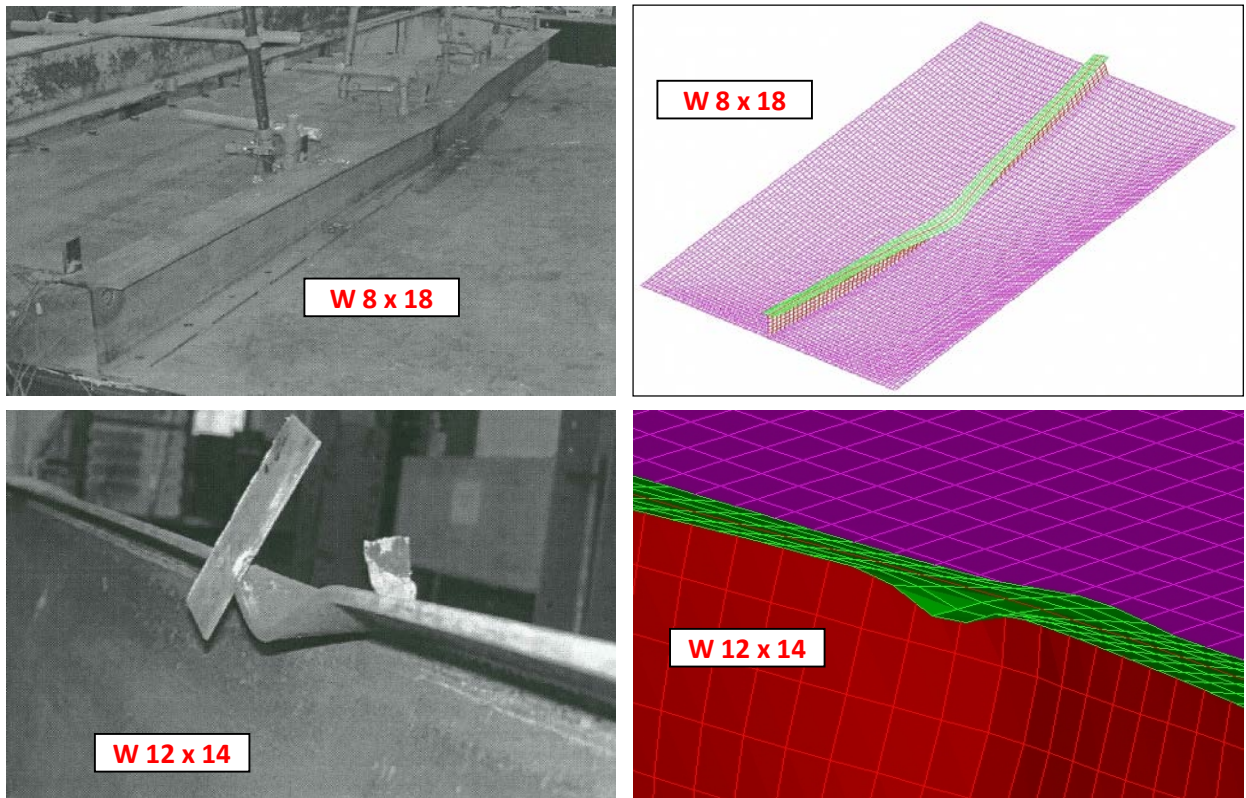
Figure 5: Comparison of Failure Modes - Experimental versus Finite Element Analysis

973

5. Concluding Remarks

Large rectangular industrial duct side panels often require regularly spaced stiffeners. Under negative pressure (suction) situation, the unconnected flange of the stiffener is in compression and the duct panel is in tension. The tension flange, which is connected to the duct panel, and the web may provide a partial rotational restraint to the compression flange of the stiffeners, thus the establishment of the bending capacity and the design of such stiffened steel panels are not straightforward. Finite element analysis models were built using the finite element software ADINA(2009). The shell element used in this study can be employed to model thick and thin general shell structures, undergoing large displacement/small strains. The material model selected for the elements was elasto-plastic-multilinear material model with von Mises yield criterion, associated flow plasticity based on isotropic hardening rule. The finite element model included reasonable geometric imperfections and residual stresses. In order to capture the onset and spread of material yielding through thickness the Newton-Cotes rule with seven integration points was used. The Load Displacement Control (LDC) method was used to capture the loading and unloading regions of the pressure load-lateral deflection response. The finite element model was validated through comparison with experimental results. The differences between the predicted bending capacities and measured capacities are 1% for the stiffener W8x18 and only 7% for the stiffener W12x14. The finite element analysis correctly established the failure modes. Based on such comparisons, it was concluded that the as built finite element analysis model can reliably establish the response of stiffened plates in the loading and in the unloading branches. The finite element model discussed in this paper was used in a parametric study which resulted in design guidelines for such industrial ducts. However, in the interest brevity, these details are not given in this paper but may be available in future publications.

6. References

ADINA , 2009, ADINA 8.5 user manual, ADINA R & D Inc, Watertown, MA, USA.

Bradford, M.A., (1999), "Distortional Buckling Strength of Elastically Restrained Monosymmetric I-beams", Thin Walled Structures, Vol. 9, pp.339-50.

Bradford, M.A., (1998) "Inelstic Buckling of I-Beams with Continuous Elastic Tension Flange Restraint", Journal of Constructional Steel Research, Vol.48, pp.63-67.

Bradford, M.A., (1988), "Buckling Strength of Deformable Momosymmetric I-Beams", Engineering Structures, Vol.10, pp.167-173.

Bradford, M.A., and Trahair, N.S.,(1981), "Distortional buckling of I-beams", J. Struct. Div., ASCE Vol.107 (ST2), pp. 355–370.

CISC, (2010), Handbook of Steel Construction, 10th Edition, Canadian Institute of Steel Construction, Markham, Ontario, Canada.

Galambos, T.V., (1998), Guide to Stability Design Criteria for Metal Structures. 5th edition. Structural Stability Council, Rolla.

Hancock, G.J., Bradford, M.A., Trahair, N.S., (1980), "Web Distortion and Flexural Torsional Buckling", Journal of Structural Engineering, ASCE , Vol.106(ST7), pp.1557-71

Kitipornchai, S. and Trahair, N.S. (1980), "Buckling Properties of Monosymmetric I-Beams", Journal of the Structural Division, ASCE, Vol.106(ST5), pp.941-957.

Svensson, S.E., (1985), "Lateral Buckling of Beams Analyzed as Elastically Supported Columns Subjected to varying Axial Force", Journal of Constructional Steel Research, Vol.5, pp.179-93.

Udall, J.D., (2007), "Effective Design of Stiffener on Industrial Ducts", Master Thesis, McMaster University, Hamilton, Canada.